

INCLUSION OF A TURBULENCE PARAMETERISATION IN A DIAGNOSTIC MASS CONSISTENT MODEL DRIVEN BY A PROGNOSTIC MODEL

Trini Castelli Silvia, Domenico Anfossi and Giovanni Belfiore

Institute of Atmospheric Sciences and Climate, National Research Council (ISAC-CNR), Torino, Italy

Abstract: Diagnostic atmospheric mass-consistent models generally are used together with turbulence parameterisations defined for flat terrain, thus in principle not able to catch the variability of the turbulence field induced by the presence of complex terrain and inhomogeneous conditions. The possibility of using prognostic turbulence fields produced accounting for the topography is then an appealing approach in inhomogeneous conditions. In this work we test an interpolation procedure applied to the turbulence fields output by a regional atmospheric model to calculate high-resolution fields, which are then coupled with the mean flow produced by a mass-consistent model. We apply this methodology to the RAMS model, using different turbulence closures, and we evaluate the feasibility of using interpolating modules paired up to MINERVE mass-consistent model.

Key words: turbulence fields, atmospheric models, diagnostic mass-consistent models, downscaling, interpolating procedures.

1. INTRODUCTION

In air pollution dispersion study and impact assessment, to reproduce the meteorology at high resolution (order of 100 m) we often apply a downscaling (Trini Castelli et al., 2007) from the prognostic mesoscale model RAMS (Pielke et al., 1992; Cotton et al., 2001) to the mass-consistent diagnostic model MINERVE (Aria Technologies, 1995). The main advantage of this approach lays in the possibility of combining the 3D gridded prognostic fields with local available measurements, and to include a more detailed topography. This allows representing both the mesoscale forcing and the peculiarities of the local flow in complex topography, providing more spatially detailed meteorological fields. The meteorological fields are then input to the Lagrangian particle dispersion model SPRAY. For its nature, MINERVE is not designed to account for the prognostic turbulence fields, and the Lagrangian turbulent variables are thus calculated in SPRAY from parameterisations defined for flat terrain.

In this work we investigate whether a proper interpolation from the coarser-resolution prognostic 3D-gridded turbulence fields, like diffusion coefficients, turbulent kinetic energy and its dissipation, might be used in complex and inhomogeneous terrain. In this way, the shortcoming of using parameterised turbulent fields might be overcome by coupling MINERVE with a module, which calculates the turbulence fields on the high-resolution diagnostic grid by interpolating from the coarser prognostic grid.

To evaluate and verify the reliability of this approach, we simulate a daily cycle in real complex terrain, then considering three combinations for the calculation of the turbulence. Firstly, we run RAMS in a configuration with four nested grids, where the third and the fourth grids have respectively 1 km and 250 m resolution. We therefore consider the RAMS fields at 250 m as the 'truth' versus which to test the other two combinations. The turbulence fields simulated in the 1-km grid are interpolated on the 250-m mesh points, originating the turbulence dataset to be checked as an alternative to flat-terrain parameterisations. At the same time, we perform a downscaling of the mean flow to 250 m with MINERVE, using in input the 1-km resolution grid RAMS fields. MINERVE wind fields at 250 m are then used to calculate the surface layer and boundary layer parameters entering the turbulence calculation in the standard configuration that is applying the Hanna (1982) parameterisation.

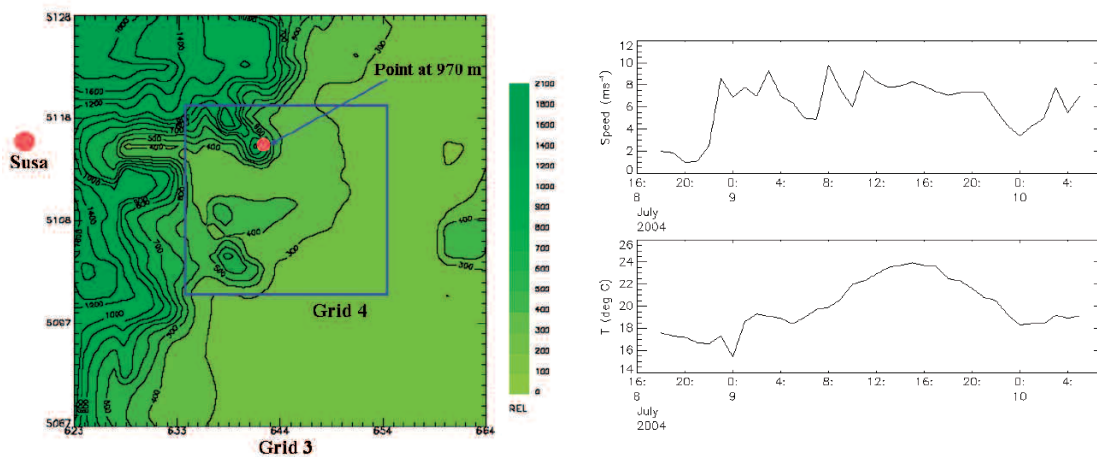


Figure 1. Grid 3 and 4 simulation domains (left) and observed wind speed and temperature in Susa (right).

Results of the comparison are discussed looking at wind velocity and turbulence fields on the full simulation domain and at single points, located in a strongly inhomogeneous topography. The sensitivity of the results versus the choice of the turbulence closure in RAMS is also considered.

2. THE CASE STUDY

To verify the possibility of using turbulence fields interpolated from a coarser grid resolution in downscaling from a prognostic to a diagnostic model, we consider and test three turbulence closures implemented in RAMS, also to investigate a possible dependence of the outputs on the grid mesh. The closures considered are the widely used Mellor-Yamada 2.5 scheme (Mellor and Yamada, 1974 and 1982, MY2.5 hereafter), a standard E-/isotropic closure (Trini Castelli et al., 2001, 2005) and a so-called “anisotropic version” of the E-/closure (Trini Castelli et al., 2006, E/-anis hereafter). The standard E-/closure describes isotropic turbulence, thus it could better represent and solve the flow and turbulence when horizontal resolutions approach the order, ~ 100 m, of the typical vertical resolution used in the atmospheric boundary layer in mesoscale modelling. On the other hand, non-isotropic closures should be more appropriate for the simulation of the atmospheric processes determined and characterized by non-homogeneous and non-isotropic conditions, and when relatively fine resolutions in the vertical are matched with large resolutions in the horizontal. We briefly recall that MY2.5 scheme solves the turbulent kinetic energy (t.k.e.) equation in the boundary layer approximation, while in E-/ and E/-anis schemes the dynamical equation of the t.k.e. is fully 3D. In RAMS, MY2.5 is used in the vertical and it is coupled with a Smagorinsky-type (1963) deformational scheme in the horizontal, based on the horizontal deformation of horizontal velocity components and on a length scale, set equal to the horizontal grid spacing Δx . An analogous combination is adopted for the E/-anis scheme, which applies the E-/closure in the vertical and the deformation scheme in the horizontal, but here the full 3D deformation of velocity components is used and the deformation length scale is calculated as $(\Delta x \Delta y \Delta z)^{1/3}$.

In this work, a real-terrain case, corresponding to a domain in the North-West Italian Alpine region around Torino (Fig. 1, left), is considered and a downscaling from the regional to the local scale is performed. The selected simulation period is a Summer day, 9 July 2004, characterized by strong convection and high wind velocity (Figure 1, right). In the numerical simulations, four nested 3D grids are used in RAMS: the largest one has a horizontal resolution of 16 km, the second one a 4 km grid-mesh, while grids 3 and 4 has respectively 1 km and 250 m grid meshes. In the vertical, 26 levels on a stretched grid are used, the first level being at 24 m height and the top of the domain at 16.5 km. The smallest domain is characterized by the presence of both almost flat terrain, around Torino city, and complex terrain, corresponding to the foot of the Alps on the West side and to the hill chain on the East side.

3. SIMULATIONS AND DISCUSSION OF RESULTS

RAMS is a widely adopted prognostic non-hydrostatic model, designed to simulate a large range of atmospheric flows from local and regional to the synoptic scale. The model includes a large number of options for the description of physical processes in atmosphere, like two-way interactive grid nesting, terrain-following coordinates, stretched vertical coordinates, nudging system, different options of numerical schemes, several top and lateral boundary conditions and a conjunct of physical parameterisations. RAMS includes also a model for soil and vegetation temperature and moisture.

The t.k.e. values obtained on the 1-km Grid-3 are interpolated with a bilinear function on the 250-m Grid-4 points. The two sets of data, referred here as Eint_G3 and E_G4, are compared through distributions, scatter diagrams and vertical profiles to evaluate the degree of accuracy of the interpolated values versus the ‘truth’ of Grid 4 data.

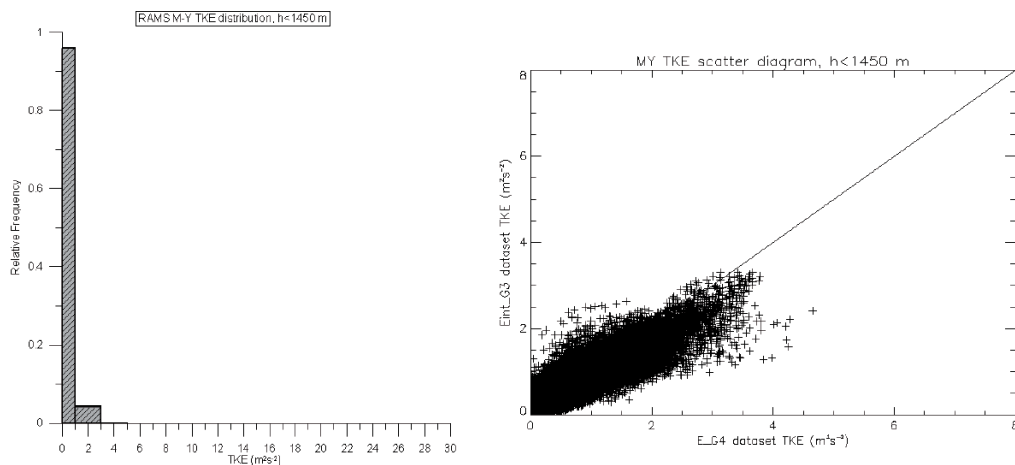


Figure 2. RAMS, MY2.5 closure, distribution (left) of Eint_G3 (dashed) and E_G4 (solid grey) t.k.e. values and their scatter diagram (right) for 24 h run up to 1450 m height.

In Figures 2-left and 3 the distributions of the t.k.e. values are reported for the 24 simulation hours in the first 1450 m for the three closures. We notice that in general MY2.5 closure is producing much lower values than E-type closures: more than 95% of MY2.5 t.k.e. values lay in the range $< 1 \text{ m}^2\text{s}^{-2}$, thus they might be not fully representative of the turbulence conditions determined by high wind velocity, convective conditions and complex terrain as those characteristics of the day here considered. E-type closures, instead, distribute in a larger range, but they also produce a small percentage of unlikely high values: worst cases occur for E-I run, where the 0.58% of E_G4 t.k.e. are $> 20 \text{ m}^2\text{s}^{-2}$, while 4.5% are $> 10 \text{ m}^2\text{s}^{-2}$. These values are produced often at the boundaries of the domains and at the nesting boundary, then in correspondence with changing orography, and are probably due to discontinuities in the flow inducing high velocity gradients, therefore high turbulence production. Moreover, high t.k.e. values occur also at heights over the boundary layer and during the night, probably generated by numerical instabilities when the turbulence quantities, determining the closure scheme, assume low threshold values. These aspects need further investigation.

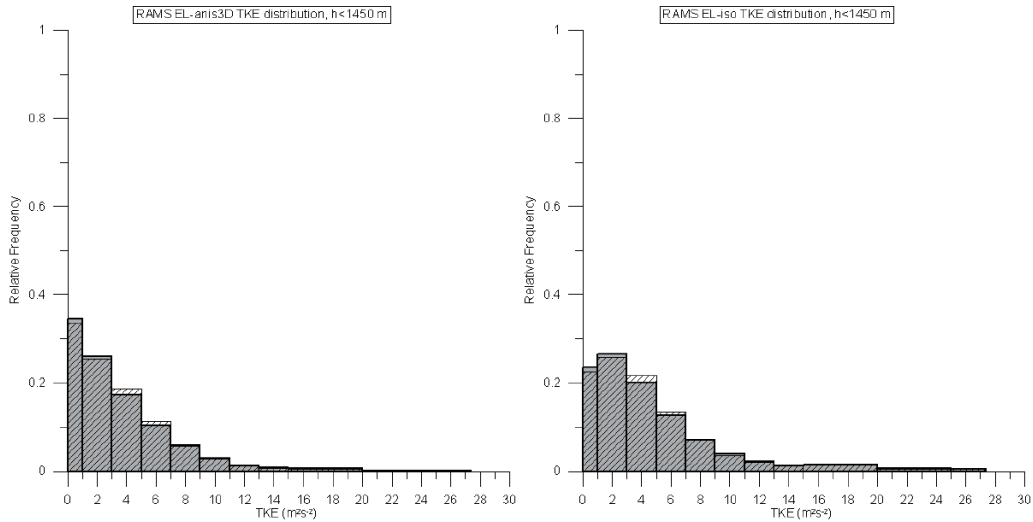


Figure 3: RAMS, distribution as in Figure 1-left, but for EI-anis (left) and EI-iso (right) closures

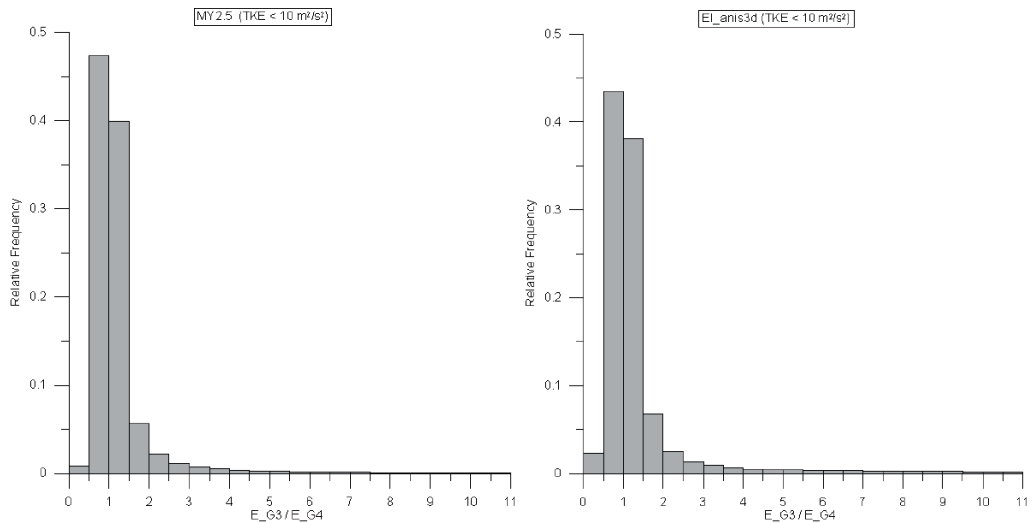


Figure 4. RAMS, distribution of the ratio of t.k.e. values ($< 10 \text{ m}^2\text{s}^{-2}$) Eint_G3/E_G4 for MY2.5 (left) and EI_anis (right) runs.

The distribution of Eint_G3 is very similar to E_G4 one in all cases, but a point to point comparison, described in Figure 2-right, as scatter diagram, and Figure 4, as distribution of the ratio of t.k.e. values Eint_G3/E_G4 for MY2.5 and EI-anis cases, reveals the differences related to the interpolating procedure. Most of ratio data are included in the range 0.5-1.5, whereas the spread between the two sets of data are probably mainly due to the fact that the Grid-3 points, from which the interpolated t.k.e. values are calculated, may be characterized by even significantly different altitudes. The agreement between Eint_G3 and E_G4 is instead less dependent on the choice of the turbulence closure scheme. Besides, the different ranges of MY2.5 and E-type t.k.e. values, in all cases the agreement is less good at the

higher values of both Eint_G3 and E_G4. In particular, in several points for E/anis, while E_G4 values reach the minimum threshold, Eint_G3 produces non negligible values, as revealed by the Eint_G3/E_G4 high-value occurrences: considering the characteristics of E/anis closure, this behaviour may be related to a sensitivity both towards the grid resolution, entering the horizontal diffusivity, and towards the use of the full 3D deformation of wind velocity.

In Figure 5 an estimate of the turbulence intensity, calculated normalizing the t.k.e. E over the speed \bar{U} as E/\bar{U}^2 , is depicted as profiles for MY2.5 (left) and E/anis (right) scheme, at a point whose altitude in Grid-4 is 970 m. The orography at the four Grid-3 points surrounding it have an altitude of 772 m (NW), 598 m (NE), 939 m (SW) and 780 m (SE), thus it corresponds to a critical location for the applicability of interpolating procedures. We choose an hour, 10 GMT (12 local time) during which MY2.5 and E/anis are producing similar wind speed profiles and the agreement of the mean flow profiles in the two Grids 3 and 4 is satisfactory, so to highlight the effect of the turbulence parameterisation and of the interpolating procedure. The RAMS Grid-3 and Grid-4 profiles are compared to the values calculated by MINERVE for the mean flow, acquiring in input the correspondent RAMS Grid-3 wind velocity, and the Hanna parameterisation for turbulence.

We notice that at this single critical point the difference between Eint_G3 and E_G4 datasets is relatively similar in the two cases, in particular the maximum of turbulence intensity is shifted at higher levels when considering the interpolated profile. The turbulence intensity is much lower in MY2.5 both than the values predicted by Hanna scheme, using the same horizontal wind field, and than E/anis values. These last are higher than the correspondent values predicted by Hanna parameterisation.

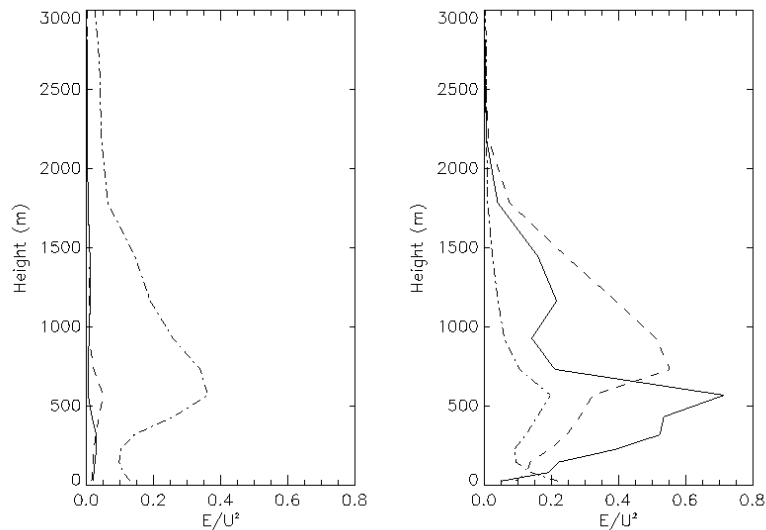


Figure 5 Estimate of turbulence intensity at a single location, for MY2.5 (left) and E/anis (right) runs. Grid-4 (solid line), interpolated Grid-3 (dashed line) and Hanna-parameterized (dot-dashed line) profiles

An example of a particularly critical situation is shown in Figure 6, corresponding to the same point as in Figure 5 but at the hour 15 GMT, where analogous stratification conditions occur for the two closures, described by the surface-layer and boundary-layer parameters reported in Table 1. In this specific hour, the wind-speed regime registered at the NE and SE points, on the lower slope of the mountain, consistently differ from that at the NW and SW points. To make a comparison with the wind speed in Grid 4, in Figure 6 we plot it together with the wind speed profile interpolated from the four Grid-3 points and the MINERVE profile. We notice that the Grid-3 interpolated for MY2.5 case, and with it the profile reproduced by MINERVE using the 1-km Grid-3 data in input, strongly differ from the Grid-4 profile; analogously it happens for the E/anis case, but with less enhanced differences. Thus the Grid-3 and MINERVE wind speed values are not representative of the speed predicted at the point in Grid 4. However, the agreement between the t.k.e. values keeps being comparable to less unfortunate cases, thus suggesting that using interpolated t.k.e. values might still be an acceptable approximation of the turbulence fields calculated at higher resolutions.

Table 1. Surface-Layer and Boundary-Layer parameters at selected point 970 m altitude, 15 GMT.

RAMS closure scheme	Friction velocity u_* (ms^{-1})	Temperature scale θ_* (K)	Monin-Obukhov length L (m)	PBL height h (m)
MY2.5	0.38	1.52	-46.01	1173.76
E/anis	0.37	1.54	-41.85	1298.38

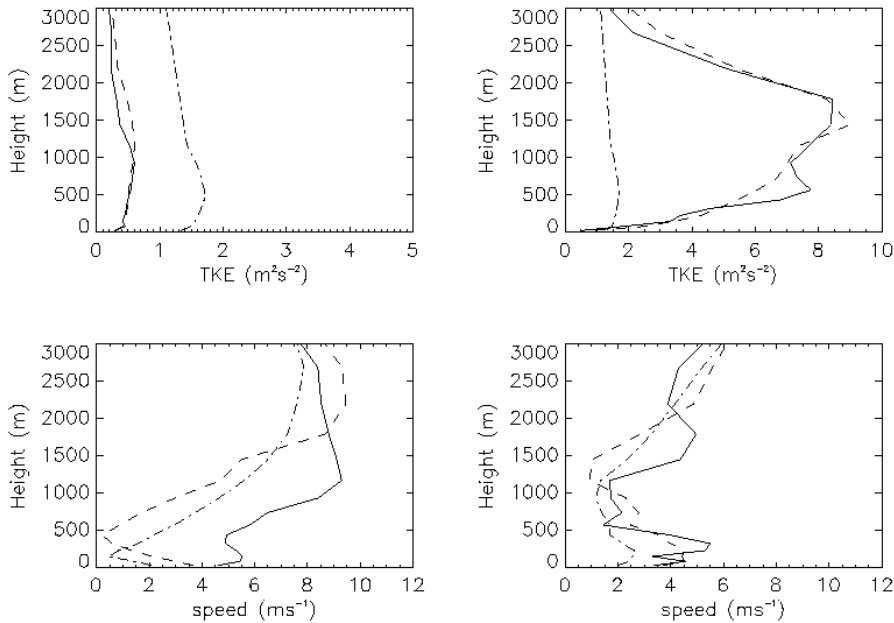


Figure 6. t.k.e. (top) and wind-speed (bottom) profiles at a single location, for MY2.5 (left) and EL anis (right) runs. Grid-4 (solid line), interpolated Grid-3 (dashed line) and Hanna-parameterized (dot-dashed line) profiles

4. CONCLUSIONS

Preliminary tests of an interpolation procedure applied on turbulence fields output by a regional atmospheric model to calculate high-resolution fields, which are then coupled with the mean flow produced by a mass-consistent model, were performed on RAMS-MINERVE downscaling system. Different closure schemes in RAMS were considered. The methodology seems to be feasible, also in complex terrain and in critical locations. Further investigations, also on the subsequent effects on the dispersion modelling, and a quantitative analysis versus observed data are under process.

REFERENCES

- Aria Technologies, 1995: Note du Principe de Modele MINERVE 4.0. Report ARIA 95.008.
- Cotton, W.R., Pielke R.A., Walko R.L., Liston G.E., Tremback C.J., Jiang H., McAnnelly R.L., Harrington J.Y., Nicholls M.E., Carrio G.G., McFadden J.P., 2003: RAMS 2001: Current status and future directions. *Meteorology and Atmospheric Physics*, **82**, 5-29.
- Hanna, S.R., 1982. Applications in air pollution modelling, Atmospheric Turbulence and Air Pollution Modelling, F.T.M. Nieuwstadt and H. Van Dop eds., Reidel, Dordrecht, 275-310.
- Mellor, G.L and T. Yamada, 1974: A Hierarchy of Turbulence Closure Models for Planetary Boundary Layers, *Journal of the Atmospheric Sciences*, **31**, 1791-1806.
- Mellor, G.L and T. Yamada, 1982: Development of a Turbulence Closure Model for Geophysical Fluid problems. *Reviews of Geophysics and Space Physics*, **20**, 851-875.
- Pielke, R.A., W.R. Cotton, R.L. Walko, C.J. Tremback, W.A. Lyons, L.D. Grasso, M.E. Nicholls, M.D. Moran, D.A. Wesley, T.J. Lee and J.H. Copeland, 1992: A Comprehensive Meteorological Modeling System – RAMS. *Meteorology and Atmospheric Physics*, **49**, 69-91.
- Smagorinsky, J., 1963: General circulation experiments with the primitive equations. *Mont. Wea. Rev.*, **91**, 99-164.
- Trini Castelli, S., E. Ferrero and D. Anfossi, 2001: Turbulence closure in neutral boundary layer over complex terrain. *Boundary-Layer Meteorology*, **100**, 405-419.
- Trini Castelli, S., E. Ferrero, D. Anfossi and R. Ohba, 2005: Turbulence closure models and their application in RAMS. *Environmental Fluid Mechanics*, **5**, 169-192.
- Trini Castelli, S., T. Hara, R. Ohba and C.J. Tremback, 2006: Validation studies of turbulence closure schemes for high resolutions in mesoscale meteorological models. *Atmospheric Environment*, **40**, 2510-2523.
- Trini Castelli, S., G. Belfiore, D. Anfossi and E. Elampe, 2007: Modelling the meteorology and traffic pollutant dispersion in highly complex terrain: the ALPNAP Alpine Space Project. *Proceedings of the 11th International Conference on Harmonisation within Atmospheric Dispersion Modelling for Regulatory Purposes*, Cambridge (United Kingdom) 2-5 July 2007, vol. 1, 225-229.